ConceptGraphs: Open-Vocabulary 3D Scene Graphs for Perception and Planning

https://concept-graphs.github.io/

Qiao Gu[†*1], Ali Kuwajerwala[†*2], Sacha Morin[*2], Krishna Murthy Jatavallabhula[*3],
Bipasha Sen[2], Aditya Agarwal[2], Kirsty Ellis[2], Celso Miguel de Melo[4],
Corban Rivera[5], William Paul[5], Rama Chellappa[6], Chuang Gan[3],
Joshua B. Tenenbaum[3], Antonio Torralba[3], Florian Shkurti[1] Liam Paull[2],
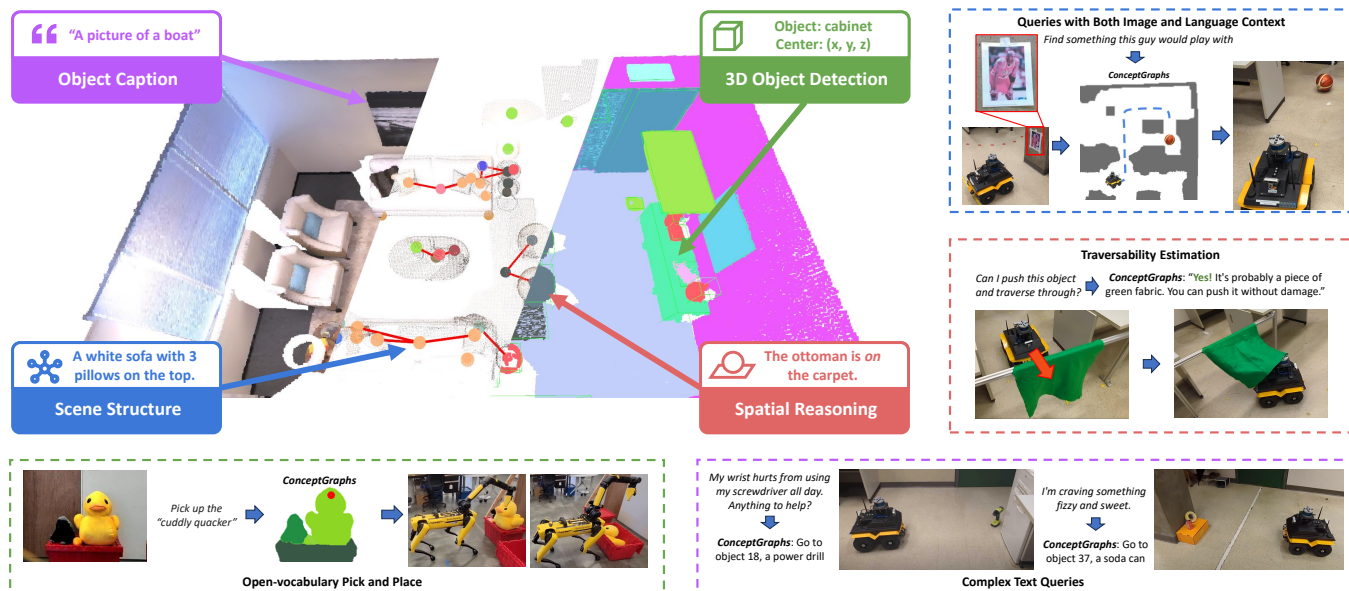[1]University of Toronto, [2]Université de Montréal, [3]MIT, [4]DEVCOM ARL, [5]JHU APL, [6]JHU

Fig. 1: *ConceptGraphs* builds open-vocabulary 3D scene graphs. We (a) design an object-based mapping system that only assumes class-agnostic instance masks and fuses them to 3D, (b) interprets and extracts language tags for each mapped instance leveraging large vision-language models, and (c) builds a graph of object spatial relationships by leveraging priors encoded in large language models. The object-centric nature of *ConceptGraphs* allows easy map maintenance and promotes scalability, and the graph structure provides relational information within the scene. Furthermore, our scene graph representations are easily mapped to natural language formats to interface with LLMs, enabling them to answer complex scene queries and granting robots access to useful facts about surrounding objects, such as traversability and utility. We implement and demonstrate *ConceptGraphs* on a number of real-world robotics tasks across wheeled and legged mobile robot platforms. (Webpage)

Abstract— For robots to perform a wide variety of tasks, they require a 3D representation of the world that is semantically rich, yet compact and efficient for task-driven perception and planning. Recent approaches have attempted to leverage features from large vision-language models to encode semantics in 3D representations. However, these approaches tend to produce maps with per-point feature vectors, which do not scale well in larger environments, nor do they contain semantic spatial relationships between entities in the environment, which are useful for downstream planning. In this work, we propose *ConceptGraphs*, an open-vocabulary graph-structured representation for 3D scenes. *ConceptGraphs* is built by leveraging 2D foundation models and fusing their output to 3D by multi-view association. The resulting representations generalize to novel semantic classes, without the need to collect large 3D datasets or finetune models. We demonstrate the utility of this representation through a number of downstream planning tasks that are specified through abstract (language) prompts and require complex reasoning over spatial and semantic concepts. To explore the full scope of our experiments and results, we encourage readers to visit our **project webpage**.

I. INTRODUCTION

Scene representation is one of the key design choices that can facilitate downstream planning for a variety of tasks, including mobility and manipulation. Robots need to build these representations online from onboard sensors as they navigate through an environment. For efficient execution of complex tasks such representations should be: *scalable and efficient to maintain*, as the volume of the scene and the duration of the robot's operation increases; *open-vocabulary*, not limited to making inferences about a set of concepts that is predefined at training time, but capable of handling new objects and concepts at inference time; and *with a flexible level of detail* to enable planning over a range of tasks, from ones that require dense geometric information for mobility and manipulation, to ones that need abstract semantic information and object-level affordance information for task planning. We propose *ConceptGraphs*, a 3D scene representation method for robot perception and planning that satisfies all the above requirements.

†Project Lead *Equal Contribution

A. Related Work

Closed-vocabulary semantic mapping in 3D. Early works reconstruct the 3D map through online algorithms like simultaneous localization and mapping (SLAM) [1]–[5] or offline methods like structure-from-motion (SfM) [6], [7]. Aside from reconstructing 3D geometry, recent works also use deep learning-based object detection and segmentation models to reconstruct the 3D scene representations with dense semantic mapping [8]–[11] or object-level decomposition [12]–[15]. While these methods achieve impressive results in mapping semantic information to 3D, they are closed-vocabulary and their applicability is limited to object categories annotated in their training datasets.

3D scene representations using foundation models. There have been significant recent efforts [16]–[30] focused on building 3D representations by leveraging *foundation models* - large, powerful models that capture a diverse set of concepts and accomplish a wide range of tasks [31]–[35]. Such models have excelled in tackling open-vocabulary challenges in 2D vision. However, they require an "internet-scale" of training data, and no 3D datasets exist yet of a comparable size. Recent works have therefore attempted to *ground* the 2D representations produced by image and language foundation models to the 3D world and show impressive results on open-vocabulary tasks, including language-guided object grounding [17], [18], [24], [26], robot manipulation [36], [37] and navigation [38], [39]. These approaches project dense per-pixel features from images to 3D to build explicit representations such as pointclouds [17]–[21] or implicit neural representations [16], [22]–[30].

However, such methods have two key limitations. First, assigning every point a semantic feature vector is highly redundant and consumes more memory than necessary, greatly limiting scalability to large scenes. Second, these dense representations do not admit an easy decomposition – this lack of structure makes them less amenable to dynamic updates to the map (crucial for robotics).

3D scene graphs. 3D scene graphs (3DSGs) address the second limitation by compactly and efficiently describing scenes with graph structures, with nodes representing objects and edges encoding inter-object relationships [40]–[44]. These approaches have enabled building real-time systems that can dynamically build up hierarchical 3D scene representations [45]–[47], and more recently shown that various robotics planning tasks can benefit from efficiency and compactness of 3DSGs [48], [49]. However, existing work on building 3D scene graphs has been confined to the closed-vocabulary setting, limiting their applicability to a small set of tasks.

B. Overview of Our Contribution

In this work, we mitigate all the aforementioned limitations and propose **ConceptGraphs**, an open-vocabulary and object-centric 3D representation for robot perception and planning. In *ConceptGraphs*, each object is represented as a node with geometric and semantic features, and relationships among objects are encoded in the graph edges. At the core of *ConceptGraphs* is an object-centric 3D mapping technique that integrates geometric cues from conventional 3D mapping systems, and semantic cues from vision and language foundation models [31], [33], [34], [50]–[52]. Objects are assigned language tags by leveraging large language models (LLMs) [32] and large vision-language models (LVLMs) [52], which provide semantically rich descriptions and enable free-form language querying, all while using off-the-shelf models (no training/finetuning). The scene graph structure allows us to efficiently represent large scenes with a low memory footprint and makes for efficient task planning.

In experiments, we demonstrate that *ConceptGraphs* is able to discover, map, and caption a large number of objects in a scene. Further, we conduct real-world trials on multiple robot platforms over a wide range of downstream tasks, including manipulation, navigation, localization, and map updates. To summarize, our key **contributions** are:

- We propose a novel object-centric mapping system that integrates geometric cues from traditional 3D mapping systems and semantic cues from 2D foundation models.
- We construct open-vocabulary 3D scene graphs; efficient and structured semantic abstractions for perception and planning.
- We implement *ConceptGraphs* on real-world wheeled and legged robotic platforms and demonstrate a number of downstream perception and planning capabilities for complex/abstract language queries.

II. METHOD

ConceptGraphs builds a compact, semantically rich representation of a 3D environment. Given a set of posed RGB-D frames, we run a class-agnostic segmentation model to obtain candidate objects, associate them across multiple views using geometric and semantic similarity measures, and instantiate nodes in a 3D scene graph. We then use an LVLM to caption each node and an LLM to infer relationships between adjoining nodes, which results in edges in the scene graph. This resultant scene graph is open-vocabulary, encapsulates object properties, and can be used for a multitude of downstream tasks including segmentation, object grounding, navigation, manipulation, localization, and remapping. The approach is illustrated in Fig. 2.

A. Object-based 3D Mapping

Object-centric 3D representation: Given a sequence of RGB-D observations $\mathcal{I} = \{I_1, I_2, \ldots, I_t\}$, *ConceptGraphs* constructs a map, a 3D scene graph, $\mathcal{M}_t = \langle \mathbf{O}_t, \mathbf{E}_t \rangle$, where $\mathbf{O}_t = \{\mathbf{o}_j\}_{j=1\ldots J}$ and $\mathbf{E}_t = \{\mathbf{e}_k\}_{k=1\ldots K}$ represent the sets of objects and edges, respectively. Each object $\mathbf{o}_j$ is characterized by a 3D point cloud $\mathbf{p}_{\mathbf{o}_j}$ and a semantic feature vector $\mathbf{f}_{\mathbf{o}_j}$. This map is built incrementally, incorporating each incoming frame $I_t = \langle I_t^{\text{rgb}}, I_t^{\text{depth}}, \theta_t \rangle$ (color image, depth image, pose) into the existing object set $\mathbf{O}_{t-1}$, by either adding to existing objects or instantiating new ones.

Class-agnostic 2D Segmentation: When processing frame I_t, a class-agnostic segmentation model $\text{Seg}(\cdot)$ is used to obtain a set of masks $\{\mathbf{m}_{t,i}\}_{i=1\ldots M} =$
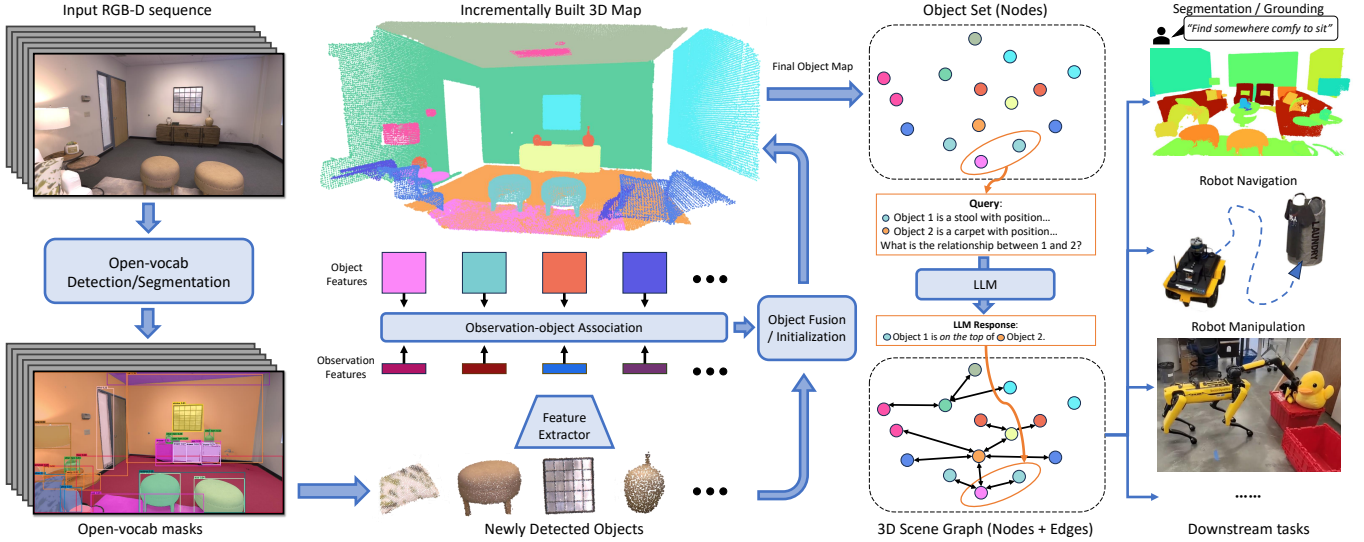
Fig. 2: *ConceptGraphs* builds an open-vocabulary 3D scene graph from a posed RGB-D video sequence. It first uses 2D foundation models to detect and segment the objects from RGB images, extracts their semantic feature vectors, and projects them into a 3D point cloud. These detections are incrementally associated and fused from multiple views, resulting in a set of 3D objects with their semantic features. Then LLMs are used to give captions to the objects and parse the relationships among them, which generates the edges to connect the set of objects and form a graph. The resulting 3D scene graph provides a structured and comprehensive understanding of the scene and can be used for various downstream tasks.

$\text{Seg}(I_t^{\text{rgb}})$ corresponding to candidate objects[1]. Each extracted mask $\mathbf{m}_{t,i}$ is then passed to a visual feature extractor (CLIP [31], DINO [50]) to obtain a visual descriptor $\mathbf{f}_{t,i} = \text{Embed}(I_t^{\text{rgb}}, \mathbf{m}_{t,i})$. Each masked region is projected to 3D, denoised using DBSCAN clustering, and transformed to the map frame. This results in a pointcloud $\mathbf{p}_{t,i}$ and its corresponding unit-normalized semantic feature vector $\mathbf{f}_{t,i}$.

Object Association: For every newly detected object $\langle \mathbf{p}_{t,i}, \mathbf{f}_{t,i} \rangle$, we compute semantic and geometric similarity with respect to all objects $\mathbf{o}_{t\text{-}1,j} = \langle \mathbf{p}_{\mathbf{o}j}, \mathbf{f}_{\mathbf{o}j} \rangle$ in the map that shares any partial geometric overlap. The geometric similarity $\phi_{\text{geo}}(i,j) = \text{nnratio}(\mathbf{p}_{t,i}, \mathbf{p}_{\mathbf{o}j})$ is the proportion of points in point cloud $\mathbf{p}_{t,i}$ that have nearest neighbors in point cloud $\mathbf{p}_{\mathbf{o}j}$, within a distance threshold of δ_{nn}. The semantic similarity $\phi_{\text{sem}}(i,j) = \mathbf{f}_{t,i}^T \mathbf{f}_{\mathbf{o}j}/2 + 1/2$ is the normalized cosine distance between the corresponding visual descriptors.[2] The overall similarity measure $\phi(i,j)$ is a sum of both: $\phi(i,j) = \phi_{\text{sem}}(i,j) + \phi_{\text{geo}}(i,j)$. We perform object association by a greedy assignment[3] strategy where each new detection is matched with an existing object with the highest similarity score. If no match is found with a similarity higher than δ_{sim}, we initialize a new object.

Object Fusion: If a detection $\mathbf{o}_{t\text{-}1,j}$ is associated with a mapped object $\mathbf{o}_j$, we fuse the detection with the map. This is achieved by updating the object semantic feature as $\mathbf{f}_{\mathbf{o}j} = (n_{\mathbf{o}j}\mathbf{f}_{\mathbf{o}j} + \mathbf{f}_{t,i})/(n_{\mathbf{o}j} + 1)$, where $n_{\mathbf{o}j}$ is the number of detections that have been associated to $\mathbf{o}_j$ so far; and

updating the pointcloud as $\mathbf{p}_{t,i} \cup \mathbf{p}_{\mathbf{o}j}$, followed by down-sampling to remove redundant points.

Node Captioning: Once the entire image sequence has been processed, a vision-language model, denoted $\text{LVLM}(\cdot)$, is used to generate object captions. For each object, the associated image crops from the *best*[4] 10 views are passed to the language model with the prompt "*describe the central object in the image*" to generate a set of initial rough captions $\hat{\mathbf{c}}_j = \{\hat{\mathbf{c}}_{j,1}, \hat{\mathbf{c}}_{j,2}, \ldots, \hat{\mathbf{c}}_{j,10}\}$ for each detected object $\mathbf{o}_j$. Each set of captions is then refined to the final caption by passing $\hat{\mathbf{c}}_j$ to another language model $\text{LLM}(\cdot)$ with a prompt instruction to summarize the initial captions into a coherent and accurate final caption $\mathbf{c}_j$.

B. Scene Graph Generation

Given the set of 3D objects $\mathbf{O}_T$ obtained from the previous step, we estimate their spatial relationships, i.e., the edges $\mathbf{E}_T$, to complete the 3D scene graph. We do this by first estimating potential connectivity among object nodes based on their spatial overlaps. We compute the 3D bounding box IoU between every pair of object nodes to obtain a similarity matrix (i.e., a dense graph), which we prune by estimating a minimum spanning tree (MST), resulting in a refined set of potential edges among the objects. To further determine the semantic relationships, for each edge in the MST, we input the information about the object pair, consisting of object captions and 3D location, to a language model LLM. The prompt instructs the model to describe the likely spatial relationship between the objects, such as "*a on b*" or "*b in a*", along with the underlying reasoning. The model outputs a relationship label with an explanation detailing the rationale. The use of an LLM allows us to extend the nominal edge

---

[1]Without loss of generality, $\text{Seg}(\cdot)$ may be replaced by open-/closed-vocabulary models to build category-specific mapping systems.

[2]For the sake of brevity, we only describe the best-performing geometric and semantic similarity measures. For an exhaustive list of alternatives, please see our project website and code.

[3]While we also experimented with optimal assignment strategies such as the Hungarian algorithm, we experimentally determined them to be slower and offer only a minuscule improvement over greedy association.

[4]We maintain a running index of the number of noise-free points each view contributes to the object point cloud.

type defined above to other output relationships a language model can interpret, such as "a backpack *may be stored in* a closet" and "sheets of paper *may be recycled in* a trash can". This results in an open-vocabulary 3D scene graph $\mathcal{M}_T = (\mathbf{O}_T, \mathbf{E}_T)$, a compact and efficient representation for use in downstream tasks.

C. Robotic Task Planning through LLMs

To enable users to carry out tasks described in natural language queries, we interface the scene graph $\mathcal{M}_T$ with an LLM. For each object in $\mathbf{O}_T$, we construct JSON-structured text descriptions that include information about its 3D location (bounding box) and its node caption. Given a text query, we task the LLM to identify the most relevant object in the scene. We then pass the 3D pose of this object to the appropriate pipeline for the downstream task (e.g., grasping, navigation). This integration of *ConceptGraphs* with an LLM is easy to implement, and enables a wide range of open-vocabulary tasks by giving robots access to the semantic properties of surrounding objects[5] (see Sec. III).

D. Implementation Details

The modularity of *ConceptGraphs* enables any appropriate open/closed-vocabulary segmentation model, LLM, or LVLM to be employed. Our experiments use Segment-Anything (SAM) [33] as the segmentation model $\mathrm{Seg}(\cdot)$, and the CLIP image encoder [31] as the feature extractor $\mathrm{Embed}(\cdot)$. We use LLaVA [52] as the vision-language model LVLM and GPT-4 [32] (gpt-4-0613) for our LLM. The voxel size for point cloud downsampling and nearest neighbor threshold δ_{nn} are both 2.5cm. We use 1.1 for the association threshold δ_{sim}.

We also develop a variant of our system, *ConceptGraphs-Detector* (*CG-D*), where we employ an image tagging model (RAM [51]) to list the object classes present in the image and an open-vocabulary 2D detector (Grounding DINO [34]) to obtain object bounding boxes[6]. In this variant, we need to separately handle detected background objects (wall, ceiling, floor) by merging them regardless of their similarity scores.

III. EXPERIMENTS

A. Scene Graph Construction

We first evaluate the accuracy of the 3D scene graphs output by the *ConceptGraphs* system in Table I. For each scene in the Replica dataset [53], we report scene graph accuracy metrics for both *CG* and the detector-variant *CG-D*. The open-vocabulary nature of our system makes automated evaluation of the quality of nodes and edges in the scene graph challenging. We instead evaluate the scene graph by engaging human evaluators on Amazon Mechanical Turk (AMT). For each node, we compute precision as the fraction of nodes for which at least 2 of 3 human evaluators deem

---

[5]For large scenes where the description length of the scene graph exceeds the context length of the LLM, one can easily substitute in alternative (concurrent) LLM planners [49].

[6]We discard the (often noisy) *tags* produced by the image tagging model, relying instead on our node captions.

---

	scene	node prec.	valid objects	duplicates	edge prec.
CG	room0	0.78	54	3	0.91
	room1	0.77	43	4	0.93
	room2	0.66	47	4	1.0
	office0	0.65	44	2	0.88
	office1	0.65	23	0	0.9
	office2	0.75	44	3	0.82
	office3	0.68	60	5	0.79
	Average	**0.71**	-	-	**0.88**
CG-D	room0	0.56	60	4	0.87
	room1	0.70	40	3	0.93
	room2	0.54	49	2	0.93
	office0	0.59	35	0	1.0
	office1	0.49	24	2	0.9
	office2	0.67	47	3	0.88
	office3	0.71	59	1	0.83
	Average	**0.61**	-	-	**0.91**

TABLE I: **Accuracy of constructed scene graphs**: node precision indicates the accuracy of the label for each node (as measured by a human evaluator); valid objects is the number of human-recognizable objects (mturkers used) discovered by our system; duplicates are the number of redundant detections; edge precision indicates the accuracy of each estimated spatial relationship (again, as evaluated by an mturker)

the node caption correct. We also report the number of valid objects retrieved by each variant by asking evaluators whether they deem each node a valid object. Both CG and CG-D identify a number of valid objects in each scene, and incur only a small number (0-5) of duplicate detections. The node labels are accurate about 70% of the time; most of the errors are incurred due to errors made by the LVLM employed (LLaVA [52]). The edges (spatial relationships) are labeled with a high degree of accuracy (90% on average).

B. 3D Semantic Segmentation

ConceptGraphs focuses on the construction of the open-vocabulary 3D scene graphs for scene understanding and planning. For completeness, in this section, we also use an open-vocabulary 3D semantic segmentation task to evaluate the quality of the obtained 3D maps. To generate the semantic segmentation, given a set of class names, we compute the similarity between the fused semantic feature of each object node and the CLIP text embeddings of the phrase an image of {class}. Then the points associated with each object are assigned to the class with the highest similarity, which gives a point cloud with dense class labels. In Table II, we report the semantic segmentation results on the Replica [53] dataset, following the evaluation protocol used in ConceptFusion [17]. We also provide an additional baseline, ConceptFusion+SAM, by replacing the Mask2Former used in ConceptFusion with the more performant SAM [33] model. As shown in Table II, the proposed *ConceptGraphs* performs comparably with or better than ConceptFusion, which has a much larger memory footprint.

C. Object Retrieval based on Text Queries

We assess the capability of *ConceptGraphs* to handle complex semantic queries, focusing on three key types.

- Descriptive: E.g., *A potted plant*.
- Affordance: E.g., *Something to use for temporarily securing a broken zipper*.

	Method	mAcc	F-mIoU
Privileged	CLIPSeg (rd64-uni) [54]	28.21	39.84
	LSeg [55]	33.39	51.54
	OpenSeg [56]	41.19	53.74
Zero-shot	MaskCLIP [57]	4.53	0.94
	Mask2former + Global CLIP feat	10.42	13.11
	ConceptFusion [17]	24.16	31.31
	ConceptFusion [17] + SAM [33]	31.53	**38.70**
	ConceptGraphs (Ours)	**40.63**	35.95
	ConceptGraphs-Detector (Ours)	38.72	35.82

TABLE II: Open-vocabulary semantic segmentation on the Replica [53] dataset. **Privileged** methods specifically finetune the pretrained models for semantic segmentation. **Zero-shot** approaches do not need any finetuning and are evaluated off the shelf.

- Negation: E.g., *Something to drink other than soda.*

We evaluate on the Replica dataset [53] and a real-world scan of the REAL Lab, where we staged a number of items including clothes, tools, and toys. For Replica, human evaluators on AMT annotate captions for SAM mask proposals, which serve as both ground truth labels and descriptive queries. We created 5 affordance and negation queries for each scene type (office & room) in Replica and 10 queries of each type for the lab scan, ensuring that each query corresponds to at least one relevant object. We manually select relevant objects as ground truth for each query.

We use two object retrieval strategies: CLIP-based and LLM-based. CLIP selects the object with the highest similarity to the query's embedding, while the LLM goes through the scenegraph nodes to identify the object with the most relevant caption. Table III shows that CLIP excels with descriptive queries but struggles with complex affordance and negation queries [58]. For example, CLIP inaccurately retrieves a backpack for the broken zipper query, whereas the LLM correctly identifies a roll of tape. The LLM performs well across the board, but is limited by the accuracy of the node captions, as discussed in Section III-A. Since the lab has a larger variety of objects to choose from, the LLM finds compatible objects for complex queries more reliably there.

D. Complex Visual-Language Queries

To assess the performance of *ConceptGraphs* in a real-world environment, we carry out navigation experiments in the REAL Lab scene with a Clearpath Jackal UGV. The robot is equipped with a VLP-16 LiDAR and a forward-facing Realsense D435i camera.

The Jackal needs to respond to abstract user queries and navigate to the most relevant object (Figure 1). By using an LVLM [52] to add a description of the current camera image to the text prompt, the robot can also answer visual queries. For example, when shown a picture of Michael Jordan and prompted with `Something this guy would play with`, the robot finds a basketball.

E. Object Search and Traversability Estimation

In this section, we showcase how the interaction between the *ConceptGraphs* representation and an LLM can enable a mobile robot to access a vast knowledge base of everyday

Dataset	Query Type	Model	R@1	R@2	R@3	# Queries
Replica	Descriptive	CLIP	0.59	0.82	0.86	20
		LLM	0.61	0.64	0.64	
	Affordance	CLIP	0.43	0.57	0.63	5
		LLM	0.57	0.63	0.66	
	Negation	CLIP	0.26	0.60	0.71	5
		LLM	0.80	0.89	0.97	
Lab	Descriptive	CLIP	1.00	–	–	10
		LLM	1.00	–	–	
	Affordance	CLIP	0.40	0.60	0.60	10
		LLM	1.00	–	–	
	Negation	CLIP	0.00	–	–	10
		LLM	1.00	–	–	

TABLE III: Object retrieval from text queries on the Replica and REAL Lab scenes. We measure the top-1, top-2, and top-3 recall. CLIP refers to object retrieval using cosine similarity, whereas LLM refers to having an LLM parse the scene graph and return the most relevant object.

objects. Specifically, we prompt an LLM to infer two additional object properties from *ConceptGraphs* captions: i) the location where a given object is typically found, and ii) if the object can be safely pushed or traversed by the Jackal robot. We design two tasks around the LLM predictions.

Object search: The robot receives an abstract user query and must navigate to the most relevant object in the *ConceptGraphs* map. Using an LVLM [52], the robot then checks if the object is at the expected location. If not, it queries an LLM to find a new plausible location given the captions of the other objects in the representation. In our prompt, we nudge the LLM to consider typical containers or storage locations. We illustrate two such queries where the target object is moved in Figure 3.

Traversability estimation: As shown in Fig. 4, we design a real-world scenario where the robot finds itself enclaved by objects. In this scenario, the robot must push around multiple objects and create a path to the goal state. While traversability can be learned through experience [59], we show that grounding LLM knowledge in a 3D map can grant similar capabilities to robotic agents.

F. Open-Vocabulary Pick and Place

To illustrate how *ConceptGraphs* can act as the perception backbone for open-vocabulary mobile manipulation, we conducted a series of experiments with a Boston Dynamics Spot Arm robot. Using an onboard RGBD camera and a *ConceptGraphs* representation of the scene, the Spot robot responds to the query `cuddly quacker` by grabbing a duck plush toy and placing it in a nearby box (Figure 1). In the supplementary video, Spot completes a similar grasping maneuver with a mango when prompted with the query `something healthy to eat`.

G. Localization and Map Updates

ConceptGraphs can also be used for object-based localization and map updates. We showcase this with a 3-DoF (x, y and yaw) localization and remapping task in the AI2Thor [60], [61] simulation environment, where a mobile robot uses a particle filter to localize in a pre-built *ConceptGraphs* map of the environment. During the

Fig. 3: A Jackal robot answering user queries using the *ConceptGraphs* representation of a lab environment. We first query an LLM to identify the most relevant object given the user query, then validate with an LVLM if the target object if is at the expected location. If not, we query the LLM again to find a likely location or container for the missing object. (Blue) When prompted with `something to wear for a space party`, the Jackal attempts to find a grey shirt with a NASA logo. After failing to detect the shirt at the expected location, the LLM reasons that it could likely be in the laundry bag. (Red) The Jackal searches for red and white sneakers after receiving the user query `footwear for a Ronald McDonald outfit`. The LLM redirects the robot to a shoe rack after failing to detect the sneakers where they initially appeared on the map.
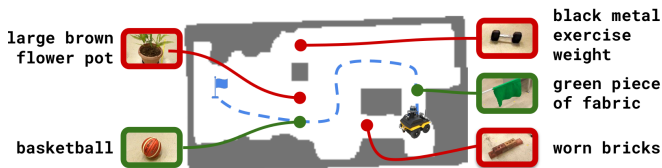

Fig. 4: The Jackal robot solving a traversability challenge. All paths to the goal are obstructed by objects. We query an LLM to identify which objects can be safely pushed or traversed by the robot (green) and which objects would be too heavy or hinder the robot's movement (red). The LLM relies on the *ConceptGraphs* node captions to make traversability predictions and we add the non-traversable objects to the Jackal costmap for path planning. The Jackal successfully reaches the goal by going through a curtain and pushing a basketball, while also avoiding contact with bricks, an iron dumbbell, and a flower pot.

observation update step of particle filtering, the robot's detections are matched against the objects in the map based on the hypothesized pose, in a similar way as described in Section II-A. The matching results are aggregated into a single observation score for weighting the pose hypothesis. During this process, previously observed objects are removed if they are not observed by the robot and new objects can also be added. We provide a demonstration of this localization and map updating approach in the supplementary video material.

H. Limitations

Despite its impressive performance, *ConceptGraphs* has failure modes that remain to be addressed in future work. First, node captioning incurs errors due to the current limitations of LVLMs like LLaVA [52]. Second, our 3D scene graph occasionally misses small or thin objects and makes duplicate detections. This impacts downstream planning, particularly when the incorrect detection is crucial to planning success. Additionally, the computational and economic costs of our system include multiple LVLM (LLaVA [52]) and one or more proprietary LLM inference(s) when building and querying the scenegraph, which may be significant.

IV. CONCURRENT WORK

We briefly review recent and unpublished pre-prints that are exploring themes related to open-vocabulary object-based factorization of 3D scenes. Concurrently to us, [62], [63] have explored open-vocabulary object-based factorization of 3D scenes. Where [62] assumes a pre-built point cloud map of the scene, [63] builds a map on the go. Both approaches associate CLIP descriptors to the reconstruction, resulting in performance comparable to our system's CLIP variant, which struggles with queries involving complex affordances and negation, as shown in Table III. OGSV [64] is closer to our setting, building an open-vocabulary 3D scene graph from RGB-D images. However, [64] relies on a (closed-set) graph neural network to predict object relationships; whereas *ConceptGraphs* relies on the capabilities of modern LLMs, eliminating the need to train an object relation model.

V. CONCLUSION

In this paper, we introduced *ConceptGraphs*, a novel approach to open-vocab object-centric 3D scene representation that addresses key limitations in the existing landscape of dense and implicit representations. Through effective integration of foundational 2D models, *ConceptGraphs* significantly mitigates memory constraints, provides relational information among objects, and allows for dynamic updates to the scene—three pervasive challenges in current methods. Experimental evidence underscores *ConceptGraphs*' robustness and extensibility, highlighting its superiority over existing baselines for a variety of real-world tasks including manipulation and navigation. The versatility of our framework also accommodates a broad range of downstream applications, thereby opening new avenues for innovation in robot perception and planning. Future work may delve into integrating temporal dynamics into the model and assessing its performance in less structured, more challenging environments.

REFERENCES

[1] R. A. Newcombe, S. Izadi, O. Hilliges, D. Molyneaux, D. Kim, A. J. Davison, P. Kohi, J. Shotton, S. Hodges, and A. Fitzgibbon, "Kinectfusion: Real-time dense surface mapping and tracking," in *IEEE international symposium on mixed and augmented reality*. IEEE, 2011, pp. 127–136. 2

[2] T. Whelan, S. Leutenegger, R. Salas-Moreno, B. Glocker, and A. Davison, "Elasticfusion: Dense slam without a pose graph," in *Robotics: Science and Systems*, 2015. 2

[3] B. Wen, J. Tremblay, V. Blukis, S. Tyree, T. Müller, A. Evans, D. Fox, J. Kautz, and S. Birchfield, "BundleSDF: Neural 6-dof tracking and 3d reconstruction of unknown objects," in *Proceedings of the IEEE/CVF Conference on Computer Vision and Pattern Recognition*, 2023, pp. 606–617. 2

[4] E. Sucar, S. Liu, J. Ortiz, and A. J. Davison, "iMAP: Implicit mapping and positioning in real-time," in *Proceedings of the IEEE/CVF International Conference on Computer Vision*, 2021, pp. 6229–6238. 2

[5] Z. Zhu, S. Peng, V. Larsson, W. Xu, H. Bao, Z. Cui, M. R. Oswald, and M. Pollefeys, "Nice-slam: Neural implicit scalable encoding for slam," in *Proceedings of the IEEE/CVF Conference on Computer Vision and Pattern Recognition*, 2022, pp. 12 786–12 796. 2

[6] J. L. Schonberger and J.-M. Frahm, "Structure-from-motion revisited," in *Proceedings of the IEEE conference on computer vision and pattern recognition*, 2016, pp. 4104–4113. 2

[7] J. L. Schönberger, E. Zheng, J.-M. Frahm, and M. Pollefeys, "Pixel-wise view selection for unstructured multi-view stereo," in *European Conference on Computer Vision*. Springer, 2016, pp. 501–518. 2

[8] J. McCormac, A. Handa, A. Davison, and S. Leutenegger, "Semanticfusion: Dense 3d semantic mapping with convolutional neural networks," in *IEEE International Conference on Robotics and automation (ICRA)*. IEEE, 2017, pp. 4628–4635. 2

[9] M. Runz, M. Buffier, and L. Agapito, "Maskfusion: Real-time recognition, tracking and reconstruction of multiple moving objects," in *IEEE International Symposium on Mixed and Augmented Reality (ISMAR)*. IEEE, 2018, pp. 10–20. 2

[10] J. McCormac, R. Clark, M. Bloesch, A. Davison, and S. Leutenegger, "Fusion++: Volumetric object-level slam," in *international conference on 3D vision (3DV)*. IEEE, 2018, pp. 32–41. 2

[11] G. Narita, T. Seno, T. Ishikawa, and Y. Kaji, "Panopticfusion: Online volumetric semantic mapping at the level of stuff and things," in *2019 IEEE/RSJ International Conference on Intelligent Robots and Systems (IROS)*. IEEE, 2019, pp. 4205–4212. 2

[12] J. Qian, V. Chatrath, J. Yang, J. Servos, A. P. Schoellig, and S. L. Waslander, "POCD: probabilistic object-level change detection and volumetric mapping in semi-static scenes," in *Robotics: Science and Systems*, K. Hauser, D. A. Shell, and S. Huang, Eds., 2022. 2

[13] J. Qian, V. Chatrath, J. Servos, A. Mavrinac, W. Burgard, S. L. Waslander, and A. P. Schoellig, "POV-SLAM: probabilistic object-aware variational SLAM in semi-static environments," in *Robotics: Science and Systems*, K. E. Bekris, K. Hauser, S. L. Herbert, and J. Yu, Eds., 2023. 2

[14] K. Li, D. DeTone, Y. F. S. Chen, M. Vo, I. Reid, H. Rezatofighi, C. Sweeney, J. Straub, and R. Newcombe, "ODAM: Object detection, association, and mapping using posed rgb video," in *Proceedings of the IEEE/CVF International Conference on Computer Vision*, 2021, pp. 5998–6008. 2

[15] M. Zins, G. Simon, and M.-O. Berger, "OA-SLAM: Leveraging objects for camera relocalization in visual slam," in *IEEE International Symposium on Mixed and Augmented Reality (ISMAR)*. IEEE, 2022, pp. 720–728. 2

[16] K. Liu, F. Zhan, J. Zhang, M. Xu, Y. Yu, A. E. Saddik, C. Theobalt, E. Xing, and S. Lu, "3d open-vocabulary segmentation with foundation models," *arXiv preprint arXiv:2305.14093*, 2023. 2

[17] K. M. Jatavallabhula, A. Kuwajerwala, Q. Gu, M. Omama, G. Iyer, S. Saryazdi, T. Chen, A. Maalouf, S. Li, N. V. Keetha, A. Tewari, J. B. Tenenbaum, C. M. de Melo, M. K. Krishna, L. Paull, F. Shkurti, and A. Torralba, "ConceptFusion: Open-set multimodal 3d mapping," in *Robotics: Science and Systems*, 2023. 2, 4, 5

[18] S. Peng, K. Genova, C. Jiang, A. Tagliasacchi, M. Pollefeys, T. Funkhouser *et al.*, "Openscene: 3d scene understanding with open vocabularies," in *Proceedings of the IEEE/CVF Conference on Computer Vision and Pattern Recognition*, 2023, pp. 815–824. 2

[19] R. Ding, J. Yang, C. Xue, W. Zhang, S. Bai, and X. Qi, "Lowis3d: Language-driven open-world instance-level 3d scene understanding," *arXiv preprint arXiv:2308.00353*, 2023. 2

[20] R. Ding, J. Yang, C. Xue, W. Zhang, S. Bai, and X. Qi, "PLA: Language-driven open-vocabulary 3d scene understanding," in *Proceedings of the IEEE/CVF Conference on Computer Vision and Pattern Recognition (CVPR)*, June 2023, pp. 7010–7019. 2

[21] J. Zhang, R. Dong, and K. Ma, "CLIP-FO3D: Learning free open-world 3d scene representations from 2d dense clip," *arXiv preprint arXiv:2303.04748*, 2023. 2

[22] V. Tschernezki, I. Laina, D. Larlus, and A. Vedaldi, "Neural feature fusion fields: 3d distillation of self-supervised 2d image representations," in *International Conference on 3D Vision (3DV)*. IEEE, 2022, pp. 443–453. 2

[23] S. Kobayashi, E. Matsumoto, and V. Sitzmann, "Decomposing nerf for editing via feature field distillation," *Advances in Neural Information Processing Systems*, vol. 35, pp. 23 311–23 330, 2022. 2

[24] N. M. M. Shafiullah, C. Paxton, L. Pinto, S. Chintala, and A. Szlam, "Clip-fields: Weakly supervised semantic fields for robotic memory," in *Robotics: Science and Systems*, K. E. Bekris, K. Hauser, S. L. Herbert, and J. Yu, Eds., 2023. 2

[25] N. Tsagkas, O. Mac Aodha, and C. X. Lu, "Vl-fields: Towards language-grounded neural implicit spatial representations," *arXiv preprint arXiv:2305.12427*, 2023. 2

[26] J. Kerr, C. M. Kim, K. Goldberg, A. Kanazawa, and M. Tancik, "LERF: Language embedded radiance fields," in *International Conference on Computer Vision (ICCV)*, 2023. 2

[27] C. Huang, O. Mees, A. Zeng, and W. Burgard, "Audio visual language maps for robot navigation," *arXiv preprint arXiv:2303.07522*, 2023. 2

[28] W. Shen, G. Yang, A. Yu, J. Wong, L. P. Kaelbling, and P. Isola, "Distilled feature fields enable few-shot manipulation," in *7th Annual Conference on Robot Learning*, 2023. [Online]. Available: https://openreview.net/forum?id=Rb0nGIt_kh5 2

[29] F. Engelmann, F. Manhardt, M. Niemeyer, K. Tateno, M. Pollefeys, and F. Tombari, "Open-set 3d scene segmentation with rendered novel views," 2023. 2

[30] K. Mazur, E. Sucar, and A. J. Davison, "Feature-realistic neural fusion for real-time, open set scene understanding," in *IEEE International Conference on Robotics and Automation (ICRA)*. IEEE, 2023, pp. 8201–8207. 2

[31] A. Radford, J. W. Kim, C. Hallacy, A. Ramesh, G. Goh, S. Agarwal, G. Sastry, A. Askell, P. Mishkin, J. Clark *et al.*, "Learning transferable visual models from natural language supervision," in *International conference on machine learning*. PMLR, 2021, pp. 8748–8763. 2, 3, 4

[32] OpenAI, "Gpt-4 technical report," *arXiv preprint arXiv:2303.08774*, 2023. 2, 4

[33] A. Kirillov, E. Mintun, N. Ravi, H. Mao, C. Rolland, L. Gustafson, T. Xiao, S. Whitehead, A. C. Berg, W.-Y. Lo *et al.*, "Segment anything," *arXiv preprint arXiv:2304.02643*, 2023. 2, 4, 5

[34] S. Liu, Z. Zeng, T. Ren, F. Li, H. Zhang, J. Yang, C. Li, J. Yang, H. Su, J. Zhu *et al.*, "Grounding dino: Marrying dino with grounded pre-training for open-set object detection," *arXiv preprint arXiv:2303.05499*, 2023. 2, 4

[35] R. Rombach, A. Blattmann, D. Lorenz, P. Esser, and B. Ommer, "High-resolution image synthesis with latent diffusion models," in *Proceedings of the IEEE/CVF conference on computer vision and pattern recognition*, 2022, pp. 10 684–10 695. 2

[36] M. Shridhar, L. Manuelli, and D. Fox, "CLIPort: What and where pathways for robotic manipulation," in *Conference on Robot Learning*, vol. 164. PMLR, 2021, pp. 894–906. 2

[37] S. Sharma, A. Rashid, C. M. Kim, J. Kerr, L. Y. Chen, A. Kanazawa, and K. Goldberg, "Language embedded radiance fields for zero-shot task-oriented grasping," in *7th Annual Conference on Robot Learning*, 2023. [Online]. Available: https://openreview.net/forum?id=k-Fg8JDQmc 2

[38] S. Y. Gadre, M. Wortsman, G. Ilharco, L. Schmidt, and S. Song, "Clip on wheels: Zero-shot object navigation as object localization and exploration," *arXiv preprint arXiv:2203.10421*, 2022. 2

[39] D. Shah, B. Osiński, S. Levine *et al.*, "Lm-nav: Robotic navigation with large pre-trained models of language, vision, and action," in *Conference on Robot Learning*. PMLR, 2023, pp. 492–504. 2

[40] M. Fisher, M. Savva, and P. Hanrahan, "Characterizing structural relationships in scenes using graph kernels," *ACM Trans. Graph.*, vol. 30, no. 4, p. 34, 2011. 2

[41] P. Gay, J. Stuart, and A. Del Bue, "Visual graphs from motion (vgfm): Scene understanding with object geometry reasoning," in *Asian Conference on Computer Vision*. Springer, 2019, pp. 330–346. 2

[42] I. Armeni, Z.-Y. He, J. Gwak, A. R. Zamir, M. Fischer, J. Malik, and S. Savarese, "3d scene graph: A structure for unified semantics, 3d space, and camera," in *Proceedings of the IEEE/CVF International Conference on Computer Vision (ICCV)*, October 2019. 2

[43] U.-H. Kim, J.-M. Park, T.-J. Song, and J.-H. Kim, "3-d scene graph: A sparse and semantic representation of physical environments for intelligent agents," *IEEE transactions on cybernetics*, vol. 50, no. 12, pp. 4921–4933, 2019. 2

[44] J. Wald, H. Dhamo, N. Navab, and F. Tombari, "Learning 3d semantic scene graphs from 3d indoor reconstructions," in *Proceedings of the IEEE/CVF Conference on Computer Vision and Pattern Recognition*, 2020, pp. 3961–3970. 2

[45] A. Rosinol, A. Violette, M. Abate, N. Hughes, Y. Chang, J. Shi, A. Gupta, and L. Carlone, "Kimera: From slam to spatial perception with 3d dynamic scene graphs," *The International Journal of Robotics Research*, vol. 40, no. 12-14, pp. 1510–1546, 2021. 2

[46] N. Hughes, Y. Chang, and L. Carlone, "Hydra: A real-time spatial perception system for 3d scene graph construction and optimization," *arXiv preprint arXiv:2201.13360*, 2022. 2

[47] S.-C. Wu, J. Wald, K. Tateno, N. Navab, and F. Tombari, "Scenegraph-fusion: Incremental 3d scene graph prediction from rgb-d sequences," in *Proceedings of the IEEE/CVF Conference on Computer Vision and Pattern Recognition*, 2021, pp. 7515–7525. 2

[48] C. Agia, K. M. Jatavallabhula, M. Khodeir, O. Miksik, V. Vineet, M. Mukadam, L. Paull, and F. Shkurti, "Taskography: Evaluating robot task planning over large 3d scene graphs," in *Conference on Robot Learning*. PMLR, 2022, pp. 46–58. 2

[49] K. Rana, J. Abou-Chakra, S. Garg, J. Haviland, I. Reid, and N. Suenderhauf, "Sayplan: Grounding large language models using 3d scene graphs for scalable task planning," in *7th Annual Conference on Robot Learning*, 2023. [Online]. Available: https://openreview.net/forum?id=wMpOMO0Ss7a 2, 4

[50] M. Oquab, T. Darcet, T. Moutakanni, H. Vo, M. Szafraniec, V. Khalidov, P. Fernandez, D. Haziza, F. Massa, A. El-Nouby *et al.*, "Dinov2: Learning robust visual features without supervision," *arXiv preprint arXiv:2304.07193*, 2023. 2, 3

[51] Y. Zhang, X. Huang, J. Ma, Z. Li, Z. Luo, Y. Xie, Y. Qin, T. Luo, Y. Li, S. Liu *et al.*, "Recognize anything: A strong image tagging model," *arXiv preprint arXiv:2306.03514*, 2023. 2, 4

[52] H. Liu, C. Li, Q. Wu, and Y. J. Lee, "Visual instruction tuning," *arXiv preprint arXiv:2304.08485*, 2023. 2, 4, 5, 6

[53] J. Straub, T. Whelan, L. Ma, Y. Chen, E. Wijmans, S. Green, J. J. Engel, R. Mur-Artal, C. Ren, S. Verma, A. Clarkson, M. Yan, B. Budge, Y. Yan, X. Pan, J. Yon, Y. Zou, K. Leon, N. Carter, J. Briales, T. Gillingham, E. Mueggler, L. Pesqueira, M. Savva, D. Batra, H. M. Strasdat, R. D. Nardi, M. Goesele, S. Lovegrove, and R. Newcombe, "The Replica dataset: A digital replica of indoor spaces," *arXiv preprint arXiv:1906.05797*, 2019. 4, 5

[54] T. Lüddecke and A. Ecker, "Image segmentation using text and image prompts," in *Proceedings of the IEEE/CVF Conference on Computer Vision and Pattern Recognition*, 2022, pp. 7086–7096. 5

[55] B. Li, K. Q. Weinberger, S. Belongie, V. Koltun, and R. Ranftl, "Language-driven semantic segmentation," in *International Conference on Learning Representations*, 2022. 5

[56] G. Ghiasi, X. Gu, Y. Cui, and T.-Y. Lin, "Scaling open-vocabulary image segmentation with image-level labels," in *European Conference on Computer Vision*. Springer, 2022, pp. 540–557. 5

[57] C. Zhou, C. C. Loy, and B. Dai, "Extract free dense labels from clip," in *European Conference on Computer Vision (ECCV)*, 2022. 5

[58] Y. Du, S. Li, and I. Mordatch, "Compositional visual generation with energy based models," in *Advances in Neural Information Processing Systems*, 2020. 5

[59] S. Levine and D. Shah, "Learning robotic navigation from experience: principles, methods and recent results," *Philosophical Transactions of the Royal Society B*, vol. 378, no. 1869, p. 20210447, 2023. 5

[60] E. Kolve, R. Mottaghi, W. Han, E. VanderBilt, L. Weihs, A. Herrasti, M. Deitke, K. Ehsani, D. Gordon, Y. Zhu *et al.*, "Ai2-thor: An interactive 3d environment for visual ai," *arXiv preprint arXiv:1712.05474*, 2017. 5

[61] M. Deitke, E. VanderBilt, A. Herrasti, L. Weihs, K. Ehsani, J. Salvador, W. Han, E. Kolve, A. Kembhavi, and R. Mottaghi, "Procthor: Large-scale embodied ai using procedural generation," *Advances in Neural Information Processing Systems*, vol. 35, pp. 5982–5994, 2022. 5

[62] A. Takmaz, E. Fedele, R. W. Sumner, M. Pollefeys, F. Tombari, and F. Engelmann, "Openmask3d: Open-vocabulary 3d instance segmentation," *arXiv preprint arXiv:2306.13631*, 2023. 6

[63] S. Lu, H. Chang, E. P. Jing, A. Boularias, and K. Bekris, "OVIR-3d: Open-vocabulary 3d instance retrieval without training on 3d data," in *7th Annual Conference on Robot Learning*, 2023. [Online]. Available: https://openreview.net/forum?id=gVBvtRqU1_ 6

[64] H. Chang, K. Boyalakuntla, S. Lu, S. Cai, E. P. Jing, S. Keskar, S. Geng, A. Abbas, L. Zhou, K. Bekris, and A. Boularious, "Context-aware entity grounding with open-vocabulary 3d scene graphs," in *7th Annual Conference on Robot Learning*, 2023. [Online]. Available: https://openreview.net/forum?id=cjEI5qXoT0 6